

Pulse separation control for mode-locked far-infrared *p*-Ge lasers

A. V. Muravjov, R. C. Strijbos, C. J. Fredricksen, S. H. Withers, and W. Trimble
Department of Physics, University of Central Florida, Orlando, Florida 32816

S. G. Pavlov and V. N. Shastin
*Institute for Physics of Microstructures, Russian Academy of Sciences, GSP-105,
 Nizhny Novgorod 603600, Russia*

R. E. Peale^{a)}
Department of Physics, University of Central Florida, Orlando, Florida 32816

(Received 8 September 1998; accepted for publication 9 November 1998)

Active mode locking of the far-infrared *p*-Ge laser giving a train of 200 ps pulses is achieved via gain modulation by applying an rf electric field together with an additional bias at one end of the crystal parallel to the Voigt-configured magnetic field. Harmonic mode locking yields a train of pulse pairs with variable time separation from zero to half the roundtrip period, where pulse separation is electrically controlled by the external bias to the rf field. © 1999 American Institute of Physics. [S0003-6951(99)02002-1]

Recent progress on *p*-Ge far-infrared lasers (50–140 cm^{-1}) includes increased duty cycle to 3%,¹ use of permanent magnets² and closed cycle refrigerators³ to eliminate liquid cryogenes, deep donor doping^{4,5} to separate impurity absorption from the gain spectrum, and active^{6–8} and passive⁹ mode locking. Motivation for these studies is a lack of compact solid-state lasers between millimeter and infrared wavelengths and increasingly important applications for THz radiation. This letter reports harmonic¹⁰ active mode locking with important new observations concerning electrical control of gain modulation and pulse separation.

Far-infrared *p*-Ge lasers operate in a wavelength range from 70 to 200 μm . Usual *p*-Ge lasers generate far-infrared pulses with a few μs duration and peak power of 1–10 W. Stimulated emission occurs on direct optical transitions between light- and heavy-hole valence subbands in bulk *p*-Ge at liquid helium temperatures in strong crossed electric and magnetic fields. Population inversion is built up at certain ratios E/B , when heavy holes repeatedly emit an optical phonon after being accelerated beyond the threshold energy ($\hbar\omega_{\text{op}} = 37$ meV), while light holes move on closed cyclotron orbits below this threshold and have a much longer lifetime. A large gain bandwidth ($\Delta\omega/\omega \sim 1$) is expected with promising consequences for tunability and short-pulse generation ($\tau_{\text{min}} \sim 1/\Delta\omega \sim \text{ps}$).¹¹

In Refs. 7 and 8, 200 ps pulses of *p*-Ge laser radiation were obtained by active mode locking with gain modulation at one end of the laser crystal, with the modulating of frequency (ν_{rf}) equal to half the cavity roundtrip frequency (ν_{RT}) (see also Ref. 6). The rf field is applied parallel to the magnetic field, and periodically accelerates light holes beyond the optical phonon threshold, upon which they are predominantly scattered to the heavy-hole band. As a consequence, the gain is expected to be modulated at the roundtrip frequency (twice per rf period), inducing mode locking. In this letter active mode locking is demonstrated for a laser

crystal with $\nu_{\text{RT}} = \nu_{\text{rf}}$. For that purpose, apparatus similar to that in Refs. 7 and 8 was developed independently but now with the additional possibility of applying an electric bias to the rf field, which allows us to control the characteristics of gain modulation and of the resulting mode-locked pulses. With this setup, generation of two pulses per roundtrip (harmonic mode locking) is achieved for the first time, and electrical control of the time delay between the pulses is demonstrated.

Single-crystal, Ga-doped, *p*-Ge with a concentration of $7 \times 10^{13} \text{ cm}^{-3}$ was cut into a rectangular bar with a cross section of $5 \times 7 \text{ mm}^2$ and a length of 84.2 mm. Ohmic contacts were made by Al evaporation and subsequent annealing at opposite lateral sides of the crystal ($5 \times L \text{ mm}^2$), and then covered with In. The crystal ends were polished parallel to each other within 1 arc minute accuracy and two external copper mirrors were attached to them via 20 μm teflon film (Fig. 1). Crystals were immersed in liquid helium at 4 K. Magnetic fields up to 1.4 T were applied in Voigt geometry using a room temperature electromagnet (Walker Scientific HF-9H) external to the cryostat (Janis 8DT). Electric field pulses E_{HV} are applied from a low duty-cycle thyatron pulser. The field orientations were $E_{\text{HV}} \parallel [1\bar{1}0]$ and $B \parallel [112]$. Radiation was conducted out of the top of the cryostat using a brass light pipe sealed with a teflon lens.

For local regulation of the orientation and fast modulation of E_{HV} , small additional contacts with a length of ~ 4 mm were placed perpendicular to the main contacts at one end of the crystal (Fig. 1) for providing an additional electric field $E_L \parallel B$. In this way, the orientation of E_{HV} can be regu-

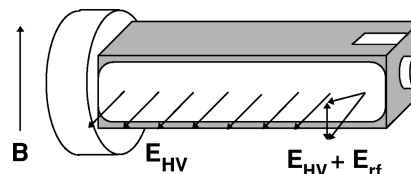


FIG. 1. Diagram of *p*-Ge laser crystal with contacts, end mirrors, applied fields, and rf electric field modulation at one end.

^{a)}Electronic mail: rep@physics.ucf.edu

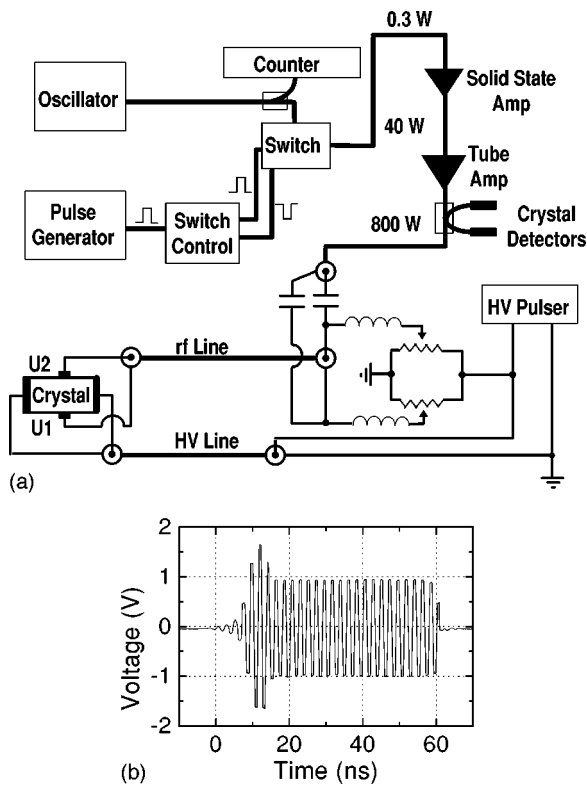


FIG. 2. (a) rf setup. Thick lines denote coaxial lines. (b) Example of (attenuated) output of the pulse-forming switch.

lated (by changing the bias) and/or modulated (by applying rf power) at one end of the laser crystal. By choosing a crystal length of 84.2 mm, the rf frequency ν_{rf} near 450 MHz of relatively cheap ham-radio electronics can be used, such that the cavity roundtrip frequency ν_{RT} equals ν_{rf} . Since the impedance of the crystal between the rf contacts is low, high rf power is required, in part to overcome the unavoidable imperfect impedance match to the dynamic load. The rf system assembled for the experiments produces clean sub- μ s pulses which just overlap the HV pulses to prevent heating of the laser crystal by the rf. Figure 2(a) presents a schematic of the rf circuit and intermediate output. The General Radio 1362 ultrahigh frequency (UHF) oscillator delivers about 0.3 W continuous wave (cw) signal that is frequency stable within a few tens of kHz. A directional coupler feeds a fraction of this signal to a Stanford Model SR620 frequency counter. The main part goes to a Minicircuits Model 15542 PIN diode switch controlled by 8 V signals from a home built controller, that itself is driven by standard TTL pulses. The (attenuated) signal after the switch is plotted in Fig. 2(b) to demonstrate the sharp rise and fall and the short pulse lengths obtainable. From the switch, low duty-cycle rf bursts enter a GE MASTR II solid-state power amplifier with gain control to give up to 40 W. This is fed to a Henry Radio Model 2004A tube amp to give up to 800 W. A Microwave Devices 318N3 directional coupler and HP 420A crystal detectors monitor forward and reflected rf power. Power measurements were verified by direct observation of the rf voltage on a fast oscilloscope. Simple isolation capacitors were used to improve impedance match to the dynamic load and protect HV and rf systems from each other. The additional bias to the rf signal is supplied by dividing the potentials U_1

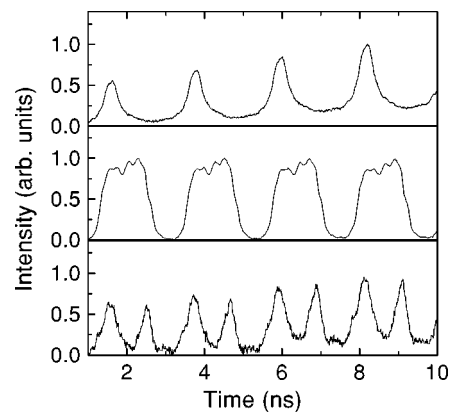


FIG. 3. Mode-locked *p*-Ge laser pulse structure for the 84.2 mm crystal. External bias added to the rf modulation increases from zero in the three frames from top to bottom.

and U_2 directly from the main high voltage pulse using two variable resistors.

Time domain detection of the laser output used a whisker-contacted Schottky-diode detector. The diode chip [1T17(82)] was purchased from the University of Virginia and the corner cube was made by Savant-Vincent, Inc., Tampa, FL. Whiskers were formed, electrolytically sharpened, and contacted to the diode by the authors. The detector was biased using a homemade battery powered current source and a Minicircuits 15542 bias-T. A Picosecond Pulse Labs 5840 amplifier with 10 GHz bandwidth boosted signals, which were then recorded on a Tektronix SCD5000 transient digitizer with 4.5 GHz analog bandwidth, 200 G-samples/s, and 11 bits vertical resolution (2 mV quantization steps).

Figure 3 shows the output of the actively mode-locked laser for different settings of the external bias ($U_1 - U_2$). The cavity roundtrip time of our 84.2-mm-long sample is calculated to be 2.20 ns giving a roundtrip frequency of $\nu_{RT} = 453.6$ MHz. Experimentally, a resonance is found at 453.8 MHz, where the applied rf is unable to extinguish lasing, indicating mode locking. Apparently, a small change in the additional bias to the rf modulation field now has a significant influence on the output of the mode-locked laser, which is now periodic at the roundtrip frequency. Increasing the offset causes the mode-locked pulses to broaden and eventually split into two. A further increase in bias causes further separation of the pulses within each pair.

This behavior is explained in Fig. 4, which shows a schematic of gain modulation and the resulting pulse train due to an rf field for three different rf offsets. In each sub-figure, the upper left curve shows the decrease of gain due to the small E_L field along the magnetic field direction. The upper right curve shows the gain modulation that results from the biased rf signal shown in the lower left corner, while the lower right bold curve shows the expected output pulse train.

When E_L [i.e., the voltage $U_1 - U_2$ in Fig. 2(a) between the additional contacts] is applied at the peak of the gain versus E_L curve [Fig. 4(c)], gain modulation occurs at twice the rf frequency, and the double pulse output from harmonic mode locking is expected. Moving the bias away from the point of maximum gain, the gain is more and more modulated at the single rf frequency, and the pulses in each pair

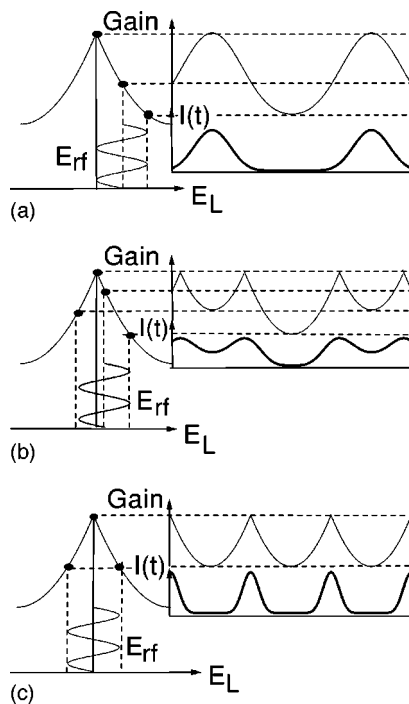


FIG. 4. Explanation of bias effects and pulse-separation control. The left curve plots gain vs external bias. The right curve shows the modulation of the gain vs time, when the rf field is applied at the bias level indicated. The pulse train expected to result is also indicated. The three situations: (a) large offset modulation far from peak of gain vs E_L , (b) small offset modulation close to peak of gain vs E_L curve, and (c) zero offset modulation at peak of gain vs E_L curve mimic the experimental results in Fig. 3.

move toward each other [Fig. 4(b)] until they are completely merged and a train of single pulses is generated [Fig. 4(a)].

A comparison of Figs. 3 and 4 shows that the experimentally observed output without any external biasing is connected to a situation where the rf modulation is already offset from the top of the gain versus E_L curve [Fig. 4(a)], and external biasing is necessary to bring the rf modulation to the top of this curve [Fig. 4(c)]. The “intrinsic” voltage offset can be shown to be due to charging of the laser crystal because of anisotropy of the hot hole distribution in the k space.⁶ For the same reason as here, external biasing was shown to enable optimization of the gain for the normal microsecond-pulse operation (without rf), and there was significant improvement in the output of an actively mode-locked p -Ge laser with $\nu_{\text{rf}} = \nu_{\text{RT}}/2$.⁶ Upon moving to the top

of the gain versus E_L curve, the total gain is optimized in the first case, while in the second the optimal situation for mode locking at twice the rf frequency is reached. A further discussion of the influence and physical origin of this offset is given in Ref. 12.

Thus, active mode locking of the p -Ge far-infrared laser with $\nu_{\text{rf}} = \nu_{\text{RT}}$ results in the generation of an output train of double far-infrared pulses with <200 ps duration (harmonic mode locking). By changing the external bias to the rf modulation field the temporal separation for a pair of mode-locked pulses can be controlled. The ability to generate a train of double pulses with electrically controllable pulse separation suggests that mode-locked p -Ge lasers may have promise for telemetry in special applications.

This work was supported by the National Science Foundation (Grant No. ECS-9531933) and AFOSR/BMDO (Grant No. F49620-97-1-0434). The coauthors from IPM thank the Russian Foundation for Basic Research (Grant No. N96-02-19275).

¹E. Bründermann, A. M. Linhart, H. P. Röser, O. D. Dubon, W. L. Hansen, and E. E. Haller, Appl. Phys. Lett. **68**, 1359 (1996).

²K. Park, R. E. Peale, H. Weidner, and J. J. Kim, IEEE J. Quantum Electron. **32**, 1203 (1996).

³E. Bründermann and H. P. Röser, Infrared Phys. Technol. **38**, 201 (1997).

⁴E. Bründermann, A. M. Linhart, L. Reichertz, H. P. Röser, O. D. Dubon, W. L. Hansen, G. Sirmain, and E. E. Haller, Appl. Phys. Lett. **68**, 3075 (1996).

⁵G. Sirmain, L. A. Reichertz, O. D. Dubon, E. E. Haller, W. L. Hansen, E. Bründermann, A. M. Linhart, and H. P. Röser, Appl. Phys. Lett. **70**, 1659 (1997).

⁶A. V. Muravjov, R. C. Strijbos, C. J. Fredricksen, H. Weidner, W. Trimble, A. Jamison, S. G. Pavlov, V. N. Shastin, and R. E. Peale, in *Radiative Processes and Dephasing in Semiconductors*, OSA-TOPS, Vol. 18, edited by D. Citron (OSA, Washington DC, 1998), pp. 102–107.

⁷J. N. Hovenier, A. V. Muravjov, S. G. Pavlov, V. N. Shastin, R. C. Strijbos, and W. Th. Wenckebach, Appl. Phys. Lett. **71**, 443 (1997).

⁸J. N. Hovenier, T. O. Klaassen, W. Th. Wenckebach, A. V. Muravjov, S. G. Pavlov, and V. N. Shastin, Appl. Phys. Lett. **72**, 1140 (1998).

⁹A. V. Muravjov, R. C. Strijbos, C. J. Fredricksen, H. Weidner, W. Trimble, S. H. Withers, S. G. Pavlov, V. N. Shastin, and R. E. Peale, Appl. Phys. Lett. **73**, 3037 (1998).

¹⁰A. E. Siegman, *Lasers* (University Science Books, Mill Valley, CA, 1986).

¹¹R. C. Strijbos, J. G. S. Lok, and W. Th. Wenckebach, J. Phys. Condens. Matter **6**, 7461 (1994).

¹²R. C. Strijbos, A. V. Muravjov, C. J. Fredricksen, W. Trimble, S. H. Withers, S. G. Pavlov, V. N. Shastin, and R. E. Peale, in *1998 IEEE Sixth International Conference on Terahertz Electronics Proceedings*, edited by P. Harrison (IEEE, Piscataway, NJ, 1998), pp. 86–89.